

# Chapter 29

## Laser Rangefinder and Monocular Camera Data Fusion for Human-Following Algorithm by PMB-2 Mobile Robot in Simulated Gazebo Environment



Elvira Chebotareva , Kuo-Hsien Hsia , Konstantin Yakovlev , and Evgeni Magid 

**Abstract** The paper presents a human-following algorithm for an autonomous mobile robot, which is equipped with a 2D laser rangefinder (LRF) and a monocular camera. As a rule, quality of a human tracking by a LRF is reduced in cluttered environments. We used a monocular camera to increase a human-tracking reliability. In contradiction with popular human-tracking algorithms that apply only a 2D LRF, our algorithm does not impose any restrictions on a type of human's clothes, and our approach does not require a human head and an upper body to be located within a monocular camera field of view. Several human trackers and variations of our algorithm were compared in the Gazebo virtual experiments within a free corridor and an office room environment. The virtual experiments demonstrated that our method successfully improved a human-tracking quality being employed with the human-following virtual PMB-2 robot.

---

E. Chebotareva (✉) · E. Magid  
Laboratory of Intelligent Robotic Systems (LIRS), Intelligent Robotics Department,  
Higher Institute for Information Technology and Intelligent Systems,  
Kazan Federal University, Kazan, Russian Federation  
e-mail: [Elvira.Chebotareva@kpfu.ru](mailto:Elvira.Chebotareva@kpfu.ru)  
URL: <https://kpfu.ru/erobotics>

E. Magid  
e-mail: [magid@it.kfu.ru](mailto:magid@it.kfu.ru)  
URL: <https://kpfu.ru/erobotics>

K.-H. Hsia  
Department of Electrical Engineering, National Yunlin University of Science  
and Technology, Douliu, Taiwan  
e-mail: [khhsia@yuntech.edu.tw](mailto:khhsia@yuntech.edu.tw)

K. Yakovlev  
Moscow Institute of Physics and Technology, Moscow, Russian Federation  
e-mail: [yakovlev@isa.ru](mailto:yakovlev@isa.ru)

© The Editor(s) (if applicable) and The Author(s), under exclusive license to Springer Nature Singapore Pte Ltd. 2021

A. Ronzhin and V. Shishlakov (eds.), *Proceedings of 15th International Conference on Electromechanics and Robotics "Zavalishin's Readings"*, Smart Innovation, Systems and Technologies 187, [https://doi.org/10.1007/978-981-15-5580-0\\_29](https://doi.org/10.1007/978-981-15-5580-0_29)

## 29.1 Introduction

The ability to follow a human is necessary for many types of assistant and companion robots. Such robots are in demand in various areas of human life. A typical example is a cargo robot that follows a human and helps to carry heavy objects, and a so-called “robotic suitcases” are already being mass-sold [8]. The concept of a robotic autonomous suitcase implies that the suitcase follows its owner, adapts to a walking pace, and avoids obstacles [18]. In RoboCup@Home competitions within “Carry My Luggage” test, a robot helps an operator to carry some luggage [24].

The ability to follow a person is important for search and rescue robots during emergencies, where a robot could follow a firefighter, which chooses a safest and easiest trajectory. Another socially significant example of human-following robots is robotic wheelchairs [26]. A capability of following a person in wheelchair does not need to be pushed, which allows an accompanying person to walk near the wheelchair, maintaining communication and visual contact with a passenger. Moreover, the ability to follow a human is critically important for social robots that interact with people through emotional communication [6].

Large number of static and dynamic objects in public spaces complicates autonomous navigation of mobile robots [21]. Presence of pedestrians makes it difficult to choose a path and can lead to a target loss. A navigation algorithm of a mobile cargo robot should simultaneously solve three problems: human detection, human tracking, and human following. A trajectory of a robot is determined by a trajectory of a target. In addition, the robot must navigate an environment, avoid collisions with obstacles and, if necessary, return to a starting point of a route [1].

2D laser rangefinders (LRF) are often used for SLAM in mobile robotics, but LRFs could also be used for human tracking. Since this tracking method is not always reliable, LRFs can be used in conjunction with visual sensors. It is economically attractive to use inexpensive monocular cameras as onboard visual sensors of a robot, which is already equipped with a LRF.

This paper presents our ongoing research on human-following problem for autonomous mobile robot PMB-2. The human-following algorithm is based on a joint use of monocular camera and LRF data. We assume that in a general case only a lower part of a human body is located within the camera’s field of view. It is important to emphasize that we avoid an approach, which assumes a strictly defined type of a target human dress, allowing to clearly distinguish two legs of a human. We also propose a universal approach of quantitative characteristics for evaluating human-following algorithms that may be useful for comparing different algorithms.

A preliminary evaluation of a human-following algorithm performance could be obtained in a simulation testing. A realistic simulator allows to reduce costs of early stages of testing and effectively prepare for real-world experiments. In this paper, for preliminary testing, we employ the 3D Gazebo simulator [17].

## 29.2 Related Work

A significant number of works have been devoted to human-following autonomous mobile robots [11]. Many models of autonomous mobile robots are equipped with LRFs, which demonstrates popularity of people tracking methods using LRFs. 2D LRF data are conveniently presented as a two-dimensional image. Since LRFs are usually placed on a small height, many methods of human tracking are based on the geometric features of searching for human legs on LRF data.

Several parameters, such as a distance between (segmented) images of two legs, leg circumference, leg thickness can be used to track human legs. Authors in [14, 27] presented methods of human detection and tracking based on a geometric approach. This approach implies that in an image from a LRF, human legs are represented in a form of two arcs or curves. Another group of methods is based on machine learning. In this case, clustering of objects separating an image of legs from a background is performed [2, 9, 20].

In addition to a LRF, various types of cameras are used for human tracking. In [7], a stereo vision-based CNN tracker for human-following robot is proposed. The work [16] is devoted to a human-following algorithm that is based on using LRF and panoramic camera data. In [19], a system of human tracking and following for robotic platforms with RGB-D camera is presented. Monocular cameras are also used as onboard sensors of human-following robots. Authors in [4] proposed a hybridizing image information based method that combines color and shape data. In [15], a target person was identified by using a combination of convolutional channel features and online boosting. Yet, onboard monocular cameras have a number of disadvantages, including limited visibility, ambiguity of scale, and detection errors. To increase the accuracy and reliability of tracking, as well as to solve other problems that arise when using service robots in cramped conditions, it is recommended to use a monocular camera in a combination with a LRF.

## 29.3 Problems of Human-Following Algorithms Implementation

We consider the following formulation of a human-following task. At a start, a human is standing in front of a robot. At a random moment, the human begins to move along an arbitrary route. The robot must follow the human at a safe distance. The robot must also avoid collisions with any obstacles. At any time, if necessary, the robot should be able to return to the starting point. At the initial time, the robot does not have information about an environment. We also assume that there are no other objects between the robot and the human at the starting time and the human is a closest visible object for the robot.

In this paper, we consider a human-following task for the PMB-2 robot by PAL Robotics [23]. The robot PMB-2 is designed for an indoors transportation of goods (up to 50 kg). The robot PMB-2 is equipped with a Hokuyo URG-04LX-UG1 LRG. For our research, we equipped PMB-2 with a monocular camera. The camera is

located at a height of 40 cm from the floor. The PMB-2 robot has a cylindrical shape with 54 cm diameter and 30 cm height. Relatively small dimensions allow the robot to move in rooms of various types, including office rooms (Fig. 29.1a). PMB-2 is navigated by ROS. The robot velocity is controlled by the *cmd\_vel* ROS package. The navigation is carried out by using *move\_base* ROS package [22].

We faced a fact that in practice, methods for detecting a human using 2D LRF are not always reliable. As an example, consider a tracker in [20]. This tracker shows good results in free spaces, but it might give false positives in cluttered spaces (Fig. 29.1). In addition, our clothing might have a significant impact on a person's visibility for the tracker. Figure 29.2 presents the data of the PMB-2 LRF as a 2D image. In Fig. 29.2a, a person in trousers is in the LRF field of view. It is clearly seen that the legs are represented as two arcs. In Fig. 29.2b, a person in a long skirt is in the LRF field of view as well. Yet, in this case, trackers based on the representation of human legs with two curves or one curve with two maximum points do not work.

Thus, in practice, there is a need to use additional sensors to track a human. The most affordable visual sensors in this case are inexpensive monocular cameras. Technical specifications of mobile robots hardware often impose restrictions on computer vision methods use. Besides, a configuration of cargo mobile robots imposes additional restrictions on a mounting height of a camera. This makes it difficult to obtain a human's full-height image. The head and upper body are important for a human detection and identification. If a camera is located at a low height, then to capture the human's head, the camera should be positioned at an angle. But in this case, the human disappears from camera's field of view when moving away from the robot. Placing the camera straight solves this problem, but in this case, at close distances, the head and upper body are not visible.

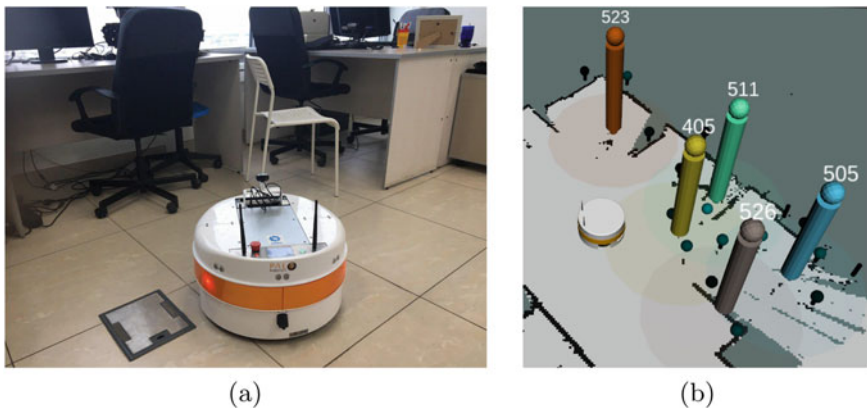


**Fig. 29.1** **a** PMB-2 robot in an office environment. **b** False positives of a leg tracker in the office environment of room 1403, Laboratory of Intelligent Robotic Systems, Kazan Federal University (KFU), 35 Kremlevskaya street, Kazan. Detected people are marked by cylinders with numerical ID labels

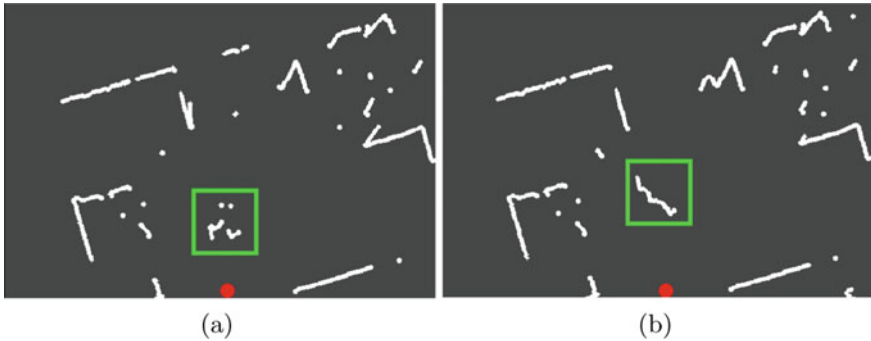


**Fig. 29.2** **a** PMB-2 robot LRF data implemented as a two-dimensional image. Inside the green square are legs of a person in trousers. The red point denotes the robot. **b** Inside the green square is a person in a long skirt

Despite a large number of works that are devoted to human-following algorithms, the algorithms evaluation and comparison are often complicated by the absence of information about qualitative and quantitative parameters. In most of the works devoted to human-following algorithms, experiments are conducted in open spaces, empty rooms, or corridors. It is natural to assume that an environment, as well as a presence of a large number of other people, can influence human-following algorithms testing results. However, in practice, checking algorithm stable work in various environments faces significant difficulties.

If tests are carried out in complex environments with people, there is a risk of a collision with people and another objects. In real environments, it is not always possible to ensure that test conditions are unchanged. Time and resources cost on the early stages of testing could be reduced with a help of simulators.

The aim of our research is to develop an approach that allows to use LRF and monocular camera data for human-following by the PMB-2 mobile robot, taking into account the problems that were described above.

## 29.4 Proposed Solution and Its Evaluation in Gazebo Simulator

This section describes an approach that allows to track a human's movement with a mobile robot using a combination of a LRF and a monocular camera. Next, the results of human-following algorithm simulation testing, which demonstrate our algorithm performance, are presented.

### 29.4.1 Evaluation of Human-Following Algorithms in Gazebo

We suggest using the Gazebo simulator at early stages of human-following algorithms development, including debugging and testing. Many popular robot models are already featured in the Gazebo with publicly available simulation packages, including the PMB-2 robot [25]. In addition, Gazebo allows creating new models of robots, populating environments with static objects (walls, furniture, etc.) and models of walking people. Therefore, Gazebo could be successfully used to test and compare prototypes of human-following algorithms. Before testing an approach in a real-world environment, we suggest constructing a model of the environment using Gazebo and evaluating a human-following algorithm within the simulated environment.

For preliminary testing, we have built 3D models of real environment of the second study building of Kazan Federal University. For experiments, we have chosen a 2.4 m width corridor (Fig. 29.3a) and  $8 \times 8$  m room (Fig. 29.3b). We had planned two types of a route for a human. In the first case, a human moved along the corridor (Fig. 29.4a). In the second case, a human started his route inside the room, left the room, and kept walking through the corridor (Fig. 29.4b). These routes contained pedestrian-specific locomotion patterns—a rectilinear movement, turning around a corner, and passing through a doorway. Each route had a length of 20 m.

To evaluate a human-following algorithm, we suggest paying a particular attention a human's velocity, a length of a successfully completed part of a route, a number of target losses, a number of human tracker false positives, a number of performed tests.



**Fig. 29.3** Experiments with the real robot PMB-2 inside the second study building of KFU, 35 Kremlevskaya street, Kazan. **a** In the corridor of the 14-th floor. **b** In the office room 1403, Laboratory of Intelligent Robotic Systems

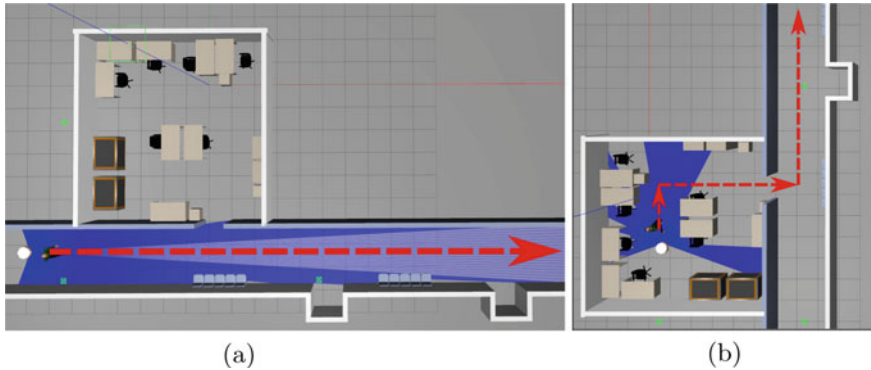


**Fig. 29.4** **a** Gazebo model of Fig. 29.3a environment. **b** Gazebo model of Fig. 29.3b environment. The long corridor corresponds to the real environment of Fig. 29.3a. The red arrow shows the human's route

### 29.4.2 Human Detection and Tracking

It is convenient to present LRF data in a form of a two-dimensional image (Fig. 29.2). As it was shown above, we cannot use geometric features of human legs for people in long clothes (e.g., a skirt or a coat).

We assume that at the algorithm initialization time, a target human is the closest object to the robot, which allows to highlight in the LRF image a region of interest (ROI) that contains a nearest curve in front of the robot. Then, this curve can be tracked using any visual tracker. We present LRF data as a 2D image of  $500 \times 500$  pixels. We connect the pairs of neighboring points by straight segments. Therefore, at the initialization time, the human is presented as a single curved line. We select the ROI so that this curve is located in its center. Knowing a scale and a position of the ROI relatively to the robot, we can calculate coordinates of a target point of the robot.

Two parameters affect the choice of a particular tracker—its accuracy and speed. To track a human in LRF data, we have compared five trackers that are released in the OpenCV library—KCF [10], TLD [13], Median Flow [12], MOSSE [5], and MIL [3]. The five trackers were tested in the Gazebo simulation of the environment shown in Fig. 29.4a. A total length of a path was 20 m with a human speed of 0.2 m/s. We conducted ten experiments for each tracker. KCF tracker immediately lost the object. TLD tracker produced false positives to other objects. Median Flow showed lost the object and produced false positives. The best results in this test were shown by MIL and MOSSE trackers. Therefore, KCF, TLD, and Median Flow trackers were not considered for further evaluation.

Next, we conducted virtual experiments on the same route with a human speed of 0.5 m/s. MOSSE tracker lost the target in ten cases out of ten, while MIL tracker successfully passed all tests not only at a speed of 0.5 m/s, but also at 1.08 m/s. Table 29.1 shows the quantitative parameters of virtual experiments results for MOSSE and

**Table 29.1** Tracker testing results

Tracker	MOSSE	MIL	MIL	MIL
Route	Corridor	Corridor	Corridor	Room
Average human speed (m/c)	0.5	0.5	1.08	0.5
Average distance travelled (m)	6.1	20	20	8.8
Number of losses	10	0	0	9
Tracker false positives	0	0	0	9
Number of experiments	10	10	10	10
Success rate (%)	0	100	100	10

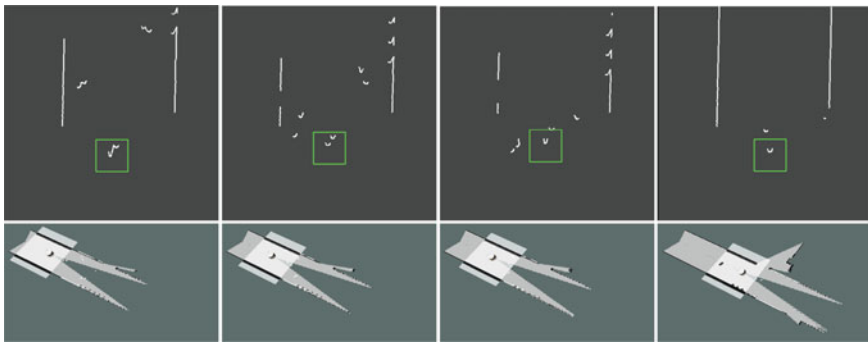


**Fig. 29.5** Tracking a human within LRF data using MIL tracker [3] (top) and the environment map constructed during the simulation in Gazebo (bottom). The tracked human legs are detected within the green square

MIL trackers. When a virtual human in the simulation walked at a speed of 1.08 m/s, we added other pedestrians to the simulation scene. Figure 29.5 presents LRF data with the target human being tracked with MIL tracker. Figure 29.5 presents the environment map, which was built by the robot while it was moving. Figure 29.6a demonstrates the simulation in Gazebo.

In addition, we conducted virtual experiments for the route shown in Fig. 29.4b. With the human speed of 0.5 m/s in nine out of ten cases, the robot with MIL tracker lost a human at corner points of the route or in a doorway. Only once the robot was able to successfully overcome both corner points, exit the doorway, and follow the human to the end of the route. The robot lost the human due to sharp turns of the trajectory. False positives were also observed when the person passed near furniture or walls.



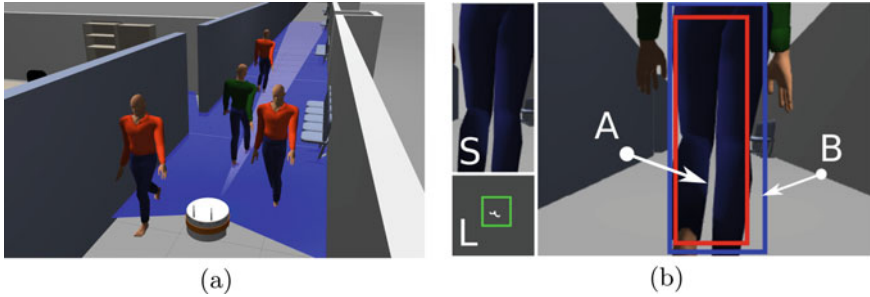


**Fig. 29.6** **a** Simulation scene. **b** Examples of areas of ROI in LRF data based image  $L$ , ROI in camera image  $A$ , initial view of the ROI in the camera image  $S$ , and the area in the camera image that the tracker defined as the human  $B$

The disadvantage of MIL tracker is a lack of information about an object loss. Additionally, we cannot reliably determine a false positive of the tracker. Therefore, we suggest using a monocular camera to control losses and false positives.

### 29.4.3 Joint Use of LRF and a Monocular Camera in a Human-Following Algorithm

In the absence of occlusions, MIL tracker provides quite accurate tracking. To control the reliability of MIL tracker, we suggest using a monocular camera. If at initialization a human simultaneously appears in the camera and LRD's fields of view, then we can fairly accurately determine the location of the person in the camera image. In this case, there is no need in human detectors. Having captured the ROI in a from a camera image, we can track the human using MIL tracker in a video stream, just like we do it on LRF data.

To detect a position of a human in initial frames of a video stream, we propose the following algorithm. In LRF data, we find a curve, which is the closest one to the robot. Using the LRF data, we trace the ROI in the camera image (so-called LRF data-based camera image area  $L$ ) to keep this curve in the center. In the camera image, we highlight the ROI (area  $A$ ) that corresponds to the LRF based ROI. We store the initial view of the ROI in the camera image (area  $S$ ), and further, this image will be used as a sample.

We associate the LRF ROI with a part of the camera image. This area will be a kind of projection of the human tracker on the image from the LRF data. Thus, at each step, we have four areas:  $L$  is the area on the image that is based on the LRF and which is defined by the tracker as the area of the human's location;  $A$  is the projection of this area onto the camera image;  $B$  is the area in the camera image that the tracker defined as the image of the human;  $S$  is the sample image of the human. Figure 29.6b demonstrates examples of  $A$ ,  $B$ ,  $S$ , and  $L$  areas. Our task is to timely

detect errors of the tracker that determines a position of a human in an image from the LRF. We also have a MIL tracker that tracks a human in the camera image. With the help of two MIL trackers, we update the areas  $B$  and  $L$ . Knowing the  $L$  area, we find the  $A$  area.

At each step of the algorithm, we calculate  $P(A = S)$  and  $P(A = B)$ , where  $P(A = S)$  is the probability that area  $A$  is a human image,  $P(A = B)$  is the probability that area  $A$  coincides with area  $B$ . In the simplest case, the correlation of the images' histograms can be taken as  $P(A = S)$  and  $P(A = B)$ . If  $P(A = S) \geq \theta_1$ , where  $\theta_1$  is a certain threshold, then we assume that the region  $L$  contains an image of the target human. If  $P(A = B) \geq \theta_2$ , where  $\theta_2$  is a certain threshold, then we assume that the area  $A$  coincides with area  $B$ . The human-following algorithm is represented in Algorithm 1. According to results of the analysis of camera and LRF data, the robot moves toward the human or begins a search of the human. Coordinates of the human are calculated based on the coordinates of the area  $L$ . The route to the human is built using a local planner.

---

#### Algorithm 1 Human-following algorithm

---

```

1:  $A =$  image of human
2:  $B = A$ 
3: while not order to return do
4:   update tracker for A
5:   update tracker for B
6:   if  $P(A = S) \geq \theta_1$  and  $P(A = B) \geq \theta_2$  then
7:     calculate the human's position
8:     move to human
9:   else
10:    while  $P(A = S) < \theta_1$  do
11:      turn
12:       $A =$  image of the nearest object (or human)
13:    end while
14:     $B = A$ 
15:   end if
16: end while

```

---

### 29.4.4 Simulation Results

We conducted two sets of ten virtual experiments demonstrating the algorithm performance for data that was obtained using a LRF and a monocular camera. The simulations were carried out for two routes (Fig. 29.4). Table 29.2 presents the simulation results for each route. For comparison, Table 29.2 shows the results of simulations when only the LRF was used for a human tracking. As we expected, in all cases, the robot successfully completed not only the route in the corridor, but also the route in the room and the corridor. Unlike previous experiments, we did not observe false positives and target losses.

**Table 29.2** Simulation results

Used sensors Route	LRF		Camera and LRF	
	Corridor	Room	Corridor	Room and corridor
Average human speed (m/s)	0.5	0.33	0.5	0.33
Average distance travelled (m)	20	13	20	20
Number of losses	0	5	0	0
Tracker false positives	0	5	0	0
Number of experiments	10	10	10	10

## 29.5 Conclusion and Future Work

In this paper, we presented a human-following algorithm based on simultaneous usage of laser rangefinder (LRF) and monocular camera data. We assumed that the camera was installed at a target human's legs level, which prevents constant tracking of such standard features as a face, an upper body or a height of a human. At the same time the algorithm does not place any restrictions on a human clothes type and is suitable for long clothes that cover legs area. Several human trackers and variations of our algorithm were compared in the Gazebo virtual experiments within a free corridor and an office room environment. The virtual experiments demonstrated that our method successfully improved a human tracking quality being employed with the human-following virtual PMB-2 robot.

As a part of our future work we will test the suggested human-following algorithm with a real PMB-2 robot in real environments that correspond to the Gazebo virtual environments, which were used in this paper.

**Acknowledgements** This research was funded by the Russian Foundation for Basic Research (RFBR), project ID 19-58-70002.

## References

1. Alishev, N., Lavrenov, R., Hsia, K.H., Su, K.L., Magid, E.: Network failure detection and autonomous return algorithms for a crawler mobile robot navigation. In: 11th International Conference on Developments in eSystems Engineering (DeSE), pp. 169–174. IEEE, New York (2018)
2. Arras, K.O., Lau, B., Grzonka, S., Luber, M., Mozos, O.M., Meyer-Delius, D., Burgard, W.: Range-based people detection and tracking for socially enabled service robots. In: Towards Service Robots for Everyday Environments, pp. 235–280. Springer, Berlin (2012)
3. Babenko, B., Yang, M.H., Belongie, S.: Visual tracking with online multiple instance learning. In: Conference on Computer Vision and Pattern Recognition, pp. 983–990. IEEE, New York (2009)

4. Bakar, M.N.A., Saad, A.R.M.: A monocular vision-based specific person detection system for mobile robot applications. *Proc. Eng.* **41**, 22–31 (2012)
5. Borgefors, G.: Distance transformations in digital images. *Comput. Vis. Graph. Image Process.* **34**(3), 344–371 (1986)
6. Chebotareva, E., Safin, R., Shafikov, A., Masaev, D., Shaposhnikov, A., Shayakhmetov, I., Gerasimov, Y., Talanov, M., Zilberman, N., Magid, E.: Emotional social robot “Emotico”. In: 12th International Conference on the Developments in eSystems Engineering, DeSE 2019 (Kazan, Russia) (2019)
7. Chen, B.X., Sahdev, R., Tsotsos, J.K.: Integrating stereo vision with a CNN tracker for a person-following robot. In: International Conference on Computer Vision Systems, pp. 300–313. Springer, Berlin (2017)
8. Cowarobot: Rover Speed. <https://cowarobotrover.com/>. Accessed on 13 Jan 2020
9. Guerrero-Higueras, Á.M., Álvarez-Aparicio, C., Olivera, M.C.C., Rodríguez-Lera, F.J., Fernández-Llamas, C., Rico, F.M., Matellán, V.: Tracking people in a mobile robot from 2D LIDAR scans using full convolutional neural networks for security in cluttered environments. *Front. Neurorobot.* **12** (2018)
10. Henriques, J.F., Caseiro, R., Martins, P., Batista, J.: Exploiting the circulant structure of tracking-by-detection with kernels. In: European Conference on Computer Vision, pp. 702–715. Springer, Berlin (2012)
11. Islam, M.J., Hong, J., Sattar, J.: Person-following by autonomous robots: a categorical overview. *Int. J. Robot. Res.* **38**(14), 1581–1618 (2019)
12. Kalal, Z., Mikolajczyk, K., Matas, J.: Forward-backward error: automatic detection of tracking failures. In: 20th International Conference on Pattern Recognition, pp. 2756–2759. IEEE, New York (2010)
13. Kalal, Z., Mikolajczyk, K., Matas, J.: Tracking-learning-detection. *IEEE Trans. Pattern Anal. Mach. Intell.* **34**(7), 1409 (2011)
14. Kawarazaki, N., Kuwae, L.T., Yoshidome, T.: Development of human following mobile robot system using laser range scanner. *Proc. Comput. Sci.* **76**, 455–460 (2015)
15. Koide, K., Miura, J., Menegatti, E.: Monocular person tracking and identification with on-line deep feature selection for person following robots. *Robot. Autonomous Syst.* **124** (2020)
16. Kristou, M., Ohya, A., Yuta, S.: Target person identification and following based on omnidirectional camera and LRF data fusion. In: RO-MAN, pp. 419–424. IEEE, New York (2011)
17. Lavrenov, R., Zakiev, A.: Tool for 3D Gazebo map construction from arbitrary images and laser scans. In: 10th International Conference on Developments in eSystems Engineering (DeSE), pp. 256–261. IEEE, New York (2017)
18. Lavrenov, R.O., Magid, E.A., Matsuno, F., Svinin, M.M., Suthakorn, J.: Development and implementation of spline-based path planning algorithm in ROS/Gazebo environment. *SPI-IRAS Proc.* **18**(1), 57–84 (2019)
19. Lee, B.J., Choi, J., Baek, C., Zhang, B.T.: Robust human following by deep Bayesian trajectory prediction for home service robots. In: International Conference on Robotics and Automation (ICRA), pp. 7189–7195. IEEE, New York (2018)
20. Leigh, A., Pineau, J., Olmedo, N., Zhang, H.: Person tracking and following with 2D laser scanners. In: International Conference on Robotics and Automation (ICRA), pp. 726–733. IEEE, New York (2015)
21. Magid, E., Lavrenov, R., Afanasyev, I.: Voronoi-based trajectory optimization for UGV path planning. In: International Conference on Mechanical, System and Control Engineering, pp. 383–387. IEEE, New York (2017)
22. Moskvina, I., Lavrenov, R.: Modeling tracks and controller for Servosila Engineer robot. In: Proceedings of 14th International Conference on Electromechanics and Robotics “Zavalishin’s Readings”, pp. 411–422. Springer, Berlin (2020)
23. Pages, J., Marchionni, L., Ferro, F.: Tiago: the modular robot that adapts to different research needs. In: International Workshop on Robot Modularity, IROS (2016)
24. RoboCup: Rules & regulations. <http://www.robocupathome.org/rules>. Accessed on 13 Jan 2020
25. ROS: Tiago base. <http://wiki.ros.org/Robots/PMB-2>. Accessed on 13 Jan 2020

26. Sato, Y., Arai, M., Suzuki, R., Kobayashi, Y., Kuno, Y., Yamazaki, K., Yamazaki, A.: A maneuverable robotic wheelchair able to move adaptively with a caregiver by considering the situation. In: RO-MAN, pp. 282–287. IEEE, New York (2013)
27. Sung, Y., Chung, W.: Hierarchical sample-based joint probabilistic data association filter for following human legs using a mobile robot in a cluttered environment. *IEEE Trans. Hum.-Mach. Syst.* **46**(3), 340–349 (2015)